Supplementary Information: Carbon Capture Turned Upside Down: High-Temperature Adsorption & Low-Temperature Desorption (HALD)

Lennart Joos, Kurt Lejaeghere, Johanna M. Huck, Veronique Van Speybroeck and Berend Smit

1 Assessing ΔS in the Langmuir Model

According to the Langmuir model we derived in the manuscript, the CO_2/H_2O selectivity is given by

$$\alpha = \frac{\theta_{CO_2}}{\theta_{H_2O}} = \frac{p_{CO_2}}{p_{H_2O}} \exp\left(-\frac{\Delta H_{ads,CO_2} - \Delta H_{ads,H_2O}}{RT}\right) \exp\left(\frac{\Delta S_{ads,CO_2} - \Delta S_{ads,H_2O}}{R}\right) \quad (1)$$

Here, we provide a more detailed treatment of the entropy term, $\Delta S_{ads,CO_2} - \Delta S_{ads,H_2O}$. To assess the entropy correctly, it is important to bear in mind the different degrees of freedom, which each have their contribution to the total entropy. An H_2O gas molecule has 3 translational, 3 rotational, and 3 vibrational degrees of freedom (Figure 1). Due to its linearity, the CO_2 molecule has 2 rotational and 4 vibrational degrees of freedom on top of 3 translations. Upon adsorption in a nanoporous materials, the molecule's translational and rotational degrees of freedom are lost and substituted by vibrational degrees of freedom that are essentially hindered translational and rotational moves.

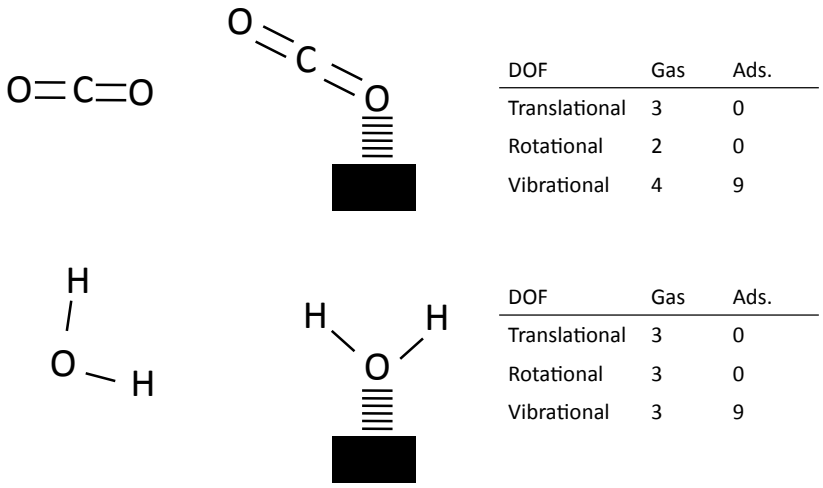

DOF	Gas	Ads.
Translational	3	0
Rotational	2	0
Vibrational	4	9

DOF	Gas	Ads.
Translational	3	0
Rotational	3	0
Vibrational	3	9

Fig. 1 The degrees of freedom (DOF) for CO_2 and H_2O in gas phase and adsorbed in a framework.

The translational, rotational and vibrational entropy contributions can be written as [1]

$$S_{trans} = k_B \ln\left(\left(\frac{2\pi k_B T}{h^2}\right)^{3/2} M^{3/2} V + 5/2\right) \tag{2}$$

$$S_{rot} = k_B \ln\left(\frac{8\pi^2}{\sigma_{rot}}\left(\frac{2\pi k_B T}{h^2}\right)^{3/2} \sqrt{I_1 I_2 I_3} + 3/2\right) \tag{3}$$

or

$$S_{rot} = k_B \ln\left(\frac{1}{\sigma_{rot}}\frac{8\pi^2 I k_B T}{h^2} + 1\right) \tag{4}$$

for a linear molecule and

$$S_{vib} = k_B \sum \frac{h\nu_i/k_B T}{e^{h\nu_i/k_B T} - 1} - \ln\left(1 - e^{-h\nu_i/k_B T}\right) \tag{5}$$

k_B is the Boltzmann constant, h Planck's constant, M the mass and V the volume of the gas molecule. σ_{rot} the symmetry number and I_x the principal moments of inertia, which are easily calculated from the atom masses and positions. Finally, ν_i, the frequencies of the vibrations are determined with DFT calculations.

The frequencies of the adsorbed molecules are assessed in zeolite unit cells with periodic boundary conditions using the Vienna Ab-initio Simulation Package[2,3]. This code uses projector-augmented wave potentials and a plane wave basis set to describe the electron density. The exchange-correlation functional is expressed by the generalized-gradient approximation with the Perdew-Burke-Ernzerhof parameterization[4,5]. The relatively large zeolite unit cells allow us to only consider the Γ point, the cut-off energy is set to 500 eV and Grimme's D3 van der Waals corrections[6] are included. The structure for MFI is taken from the IZA database[7] and the structure of –OKO from Verheyen et al.[8] The framework is kept fixed, while the gas molecules are allowed to relax until 0.01 eV/Å force convergence is reached. Frequency calculations then use 0.02 Å perturbations, leading to the obtained vibrational frequencies listed in Table 1.

H_2O@MFI ν_i (THz)	CO_2@MFI ν_i (THz)	H_2O@–OKO ν_i (THz)
114.3	70.8	113.3
111.2	39.5	102.9
47.7	19.0	47.8
8.2	18.9	19.5
7.3	3.1	14.8
5.0	2.5	6.0
2.7	2.3	6.0
2.3	1.5	4.8
1.1	0.9	2.7

Table 1 Vibrational frequencies for molecules adsorbed in zeolite frameworks.

The frequencies of the gas phase molecules were determined in Gaussian[9] to avoid imaginary frequencies that occur when gas molecules are considered with a periodic approach. The B3LYP functional and 6-31+G(d,p) basisset were used and the frequencies are shown in Table 2.

We have evaluated the difference in adsorption entropy between CO_2 and H_2O with four different approaches.

$H_2O_{(g)}$ ν_i (THz)	$CO_{2(g)}$ ν_i (THz)
117.9	72.3
114.3	40.9
48.1	19.5
	19.5

Table 2 Vibrational frequencies for gas phase H_2O and CO_2 molecules.

1.1 Model 1

In a first approximation, the adsorption entropy could be approximated by the loss in translational and rotational entropy, i.e.

$$\Delta S_{ads} = -S_{trans} - S_{rot} \tag{6}$$

The resulting adsorption entropy for CO_2 is more negative than for H_2O, i.e. $\Delta S_{ads,CO_2} - \Delta S_{ads,H_2O} < 0$ (Table 3). The main reason is that the molecular mass of CO_2 (44 g/mol) is much larger than that of H_2O (18 g/mol). The entropic term in Equation 1 will be small, resulting in low CO_2/H_2O selectivities.

ΔS_{ads}(J/molK)	CO_2	H_2O	ΔS
300 K	-210.95	-194.63	-16.32
400 K	-219.33	-204.20	-15.13

Table 3 Adsorption entropy (in J/molK) for CO_2 and H_2O assuming $\Delta S_{ads} = -S_{trans} - S_{rot}$.

1.2 Model 2

In the second model, we don't make any prior assumptions and we calculate the adsorption entropy straightforwardly as:

$$\Delta S_{ads} = S_{vib,ads} - S_{vib,gas} - S_{trans,gas} - S_{rot,gas} \tag{7}$$

The entropy of the adsorbed CO_2 and H_2O molecules ($S_{vib,ads}$) is determined in an adsorption site of the MFI framework (see Figure 2). Table 4 shows that also for this approach, the entropy loss for CO_2 is bigger than for H_2O, although the difference is negligible.

ΔS_{ads}(J/molK)	CO_2 MFI	H_2O MFI	ΔS
300 K	-119.46	-118.78	-0.68
400 K	-115.84	-115.02	-0.82

Table 4 Adsorption entropy (in J/molK) for CO_2 and H_2O in the MFI framework, with $\Delta S_{ads} = S_{vib,ads} - S_{vib,gas} - S_{trans,gas} - S_{rot,gas}$

1.3 Model 3

We show in the main manuscript (Section 4) that H_2O preferably adsorbs in a network of H_2O molecules that is already present in the framework. A single H_2O molecule in the MFI framework is therefore not a

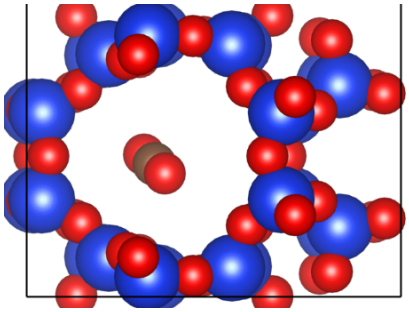

(a) CO_2 in MFI

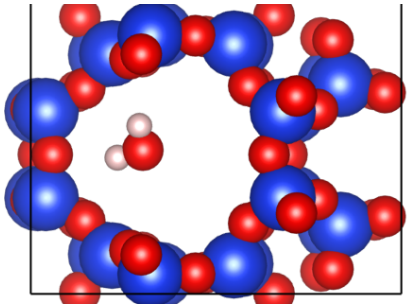

(b) H_2O in MFI

Fig. 2 Adsorption in the MFI framework

representative situation for H_2O in zeolites. To mimic the presence of a H_2O network, we now consider H_2O adsorption in the systematically interrupted –OKO zeolite, that has four –OH groups pointing into the 12-membered ring.[8] Figure 3 shows that in this framework, H_2O is strongly coordinated with hydrogen bridges. When considering the entropy of adsorbed H_2O in –OKO and the entropy of adsorbed CO_2 in MFI, the difference in the adsorption entropy between CO_2 and H_2O is positive (Table 5). This means that H_2O loses additional entropy due to the stronger interactions with other –OH groups.

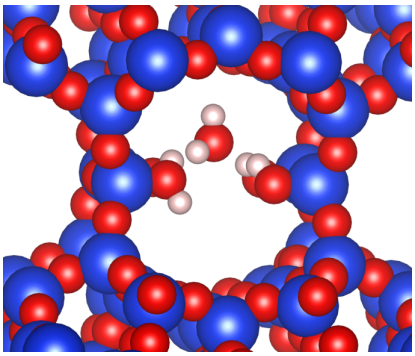

Fig. 3 Adsorption of H_2O in the –OKO framework, where it coordinates strongly with the -OH groups.

ΔS_{ads}(J/molK)	CO_2 MFI	H_2O –OKO	ΔS
300 K	-119.46	-146.24	26.78
400 K	-115.84	-143.57	27.73

Table 5 Adsorption entropy (in J/molK) for CO_2 in the MFI framework and H_2O in the –OKO framework

1.4 Model 4

Following the train of thought that H_2O loses more rotational entropy upon adsorption than does CO_2, we could also assume that CO_2 mainly loses its translational freedom whereas H_2O loses both its translational and rotational freedom. We can write this as:

$$\Delta S_{ads,CO_2} = -S_{trans,CO_2} \tag{8}$$

$$\Delta S_{ads,H_2O} = -S_{trans,H_2O} - S_{rot,H_2O} \tag{9}$$

The resulting entropy difference Δ in Table 6 is even more positive than in Table 5. The effect on the overall CO_2/H_2O selectivity (Equation 1) will therefore also be more pronounced.

ΔS_{ads}(J/molK)	CO_2	H_2O	ΔS
300 K	-156.08	-194.63	38.56
400 K	-162.06	-204.20	42.15

Table 6 Adsorption entropy (in J/molK) for CO_2 and H_2O assuming $\Delta S_{ads,CO_2} = -S_{trans,CO_2}$ and $\Delta S_{ads,H_2O} = -S_{trans,H_2O} - S_{rot,H_2O}$.

1.5 Comparison and Conclusion

In Figure 4, the four proposed theoretical models are compared with the results from molecular simulations of the binary mixtures in the zeolites of the IZA database (see Main Manuscript, Section 5). Model 2, considering both H_2O and CO_2 vibrations in MFI, fits well to the materials in the region with $\alpha_{CO_2/H_2O,400K-300K} < 0$. The corresponding materials generally have small pores that can contain only 1 CO_2 or 1 H_2O molecule, which explains the good fit with a model that compares the entropy of 1 CO_2 molecule in MFI with the entropy of 1 H_2O molecule in MFI.

For Model 3, with CO_2 and H_2O vibrations determined in MFI and –OKO respectively, the agreement at low ΔH's is worse than for Model 2, but the qualitative trend of an optimal performing region around +2 kJ/mol is visible. The discrepancy between the last points and the theoretical curve indicates the failure of the Langmuir model. This is most likely due to the fact that there are many more adsorption sites for H_2O than for CO_2, partly driven by the formation of H_2O networks

Model 4 finally, shows the same trend as Model 3, but overshoots the simulation results.

To conclude the assessment of the entropy, we decide to use the adsorption entropy for CO_2 in MFI and for H_2O in –OKO. This approach best fits the trends we also see in the molecular simulations. This in turn means that for a good fit of the theoretical model to the simulation data, the formation of H_2O networks and the associated rotational freezing of the H_2O molecule is an important factor in the adsorption entropy, as well as in the resulting CO_2/H_2O selectivity.

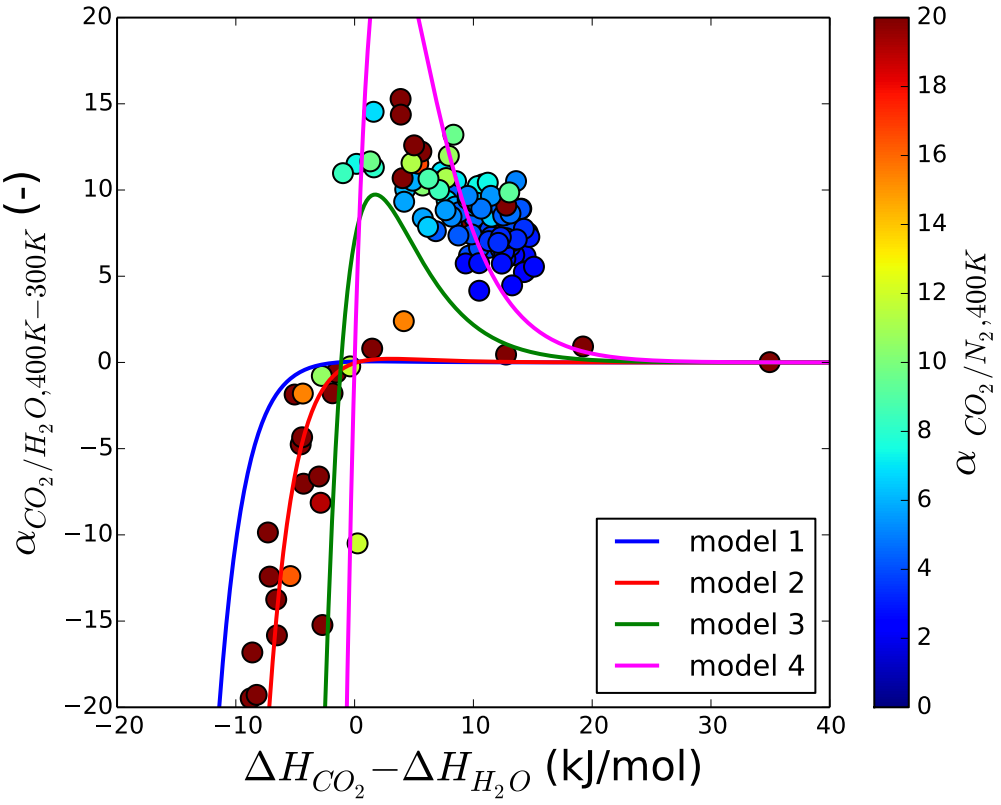

Fig. 4 Comparison of the different entropy models with the molecular simulations on the IZA database.

2 Temperature Dependence of Enthalpy and Entropy

In Figure 3 of the main manuscript, we assume that the enthalpy and entropy are constant in the 300 K - 400 K range. Figure 5 shows that this is indeed a fair assumption. The adsorption enthalpies on the one hand are taken from NVT Monte-Carlo simulations and deviate less than 0.5 kJ/mol in the considered temperature interval. The adsorption entropies on the other hand are calculated from the expressions in Model 3 and are only slightly increasing as a function of the temperature.

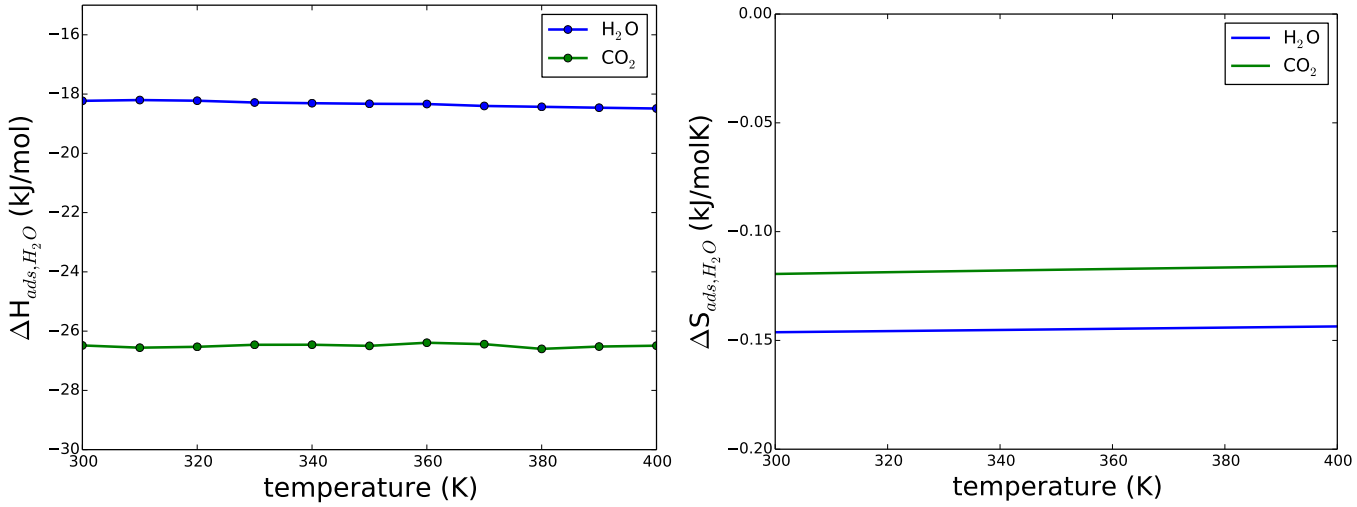

(a) Adsorption enthalpy

(b) Adsorption entropy

Fig. 5 Temperature dependence of the adsorption enthalpy and entropy for CO_2 and H_2O.

3 Pure CO_2 Adsorption Isotherms in MFI

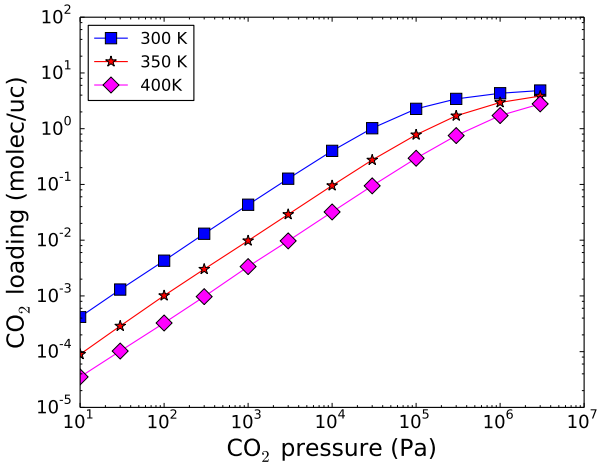

Fig. 6 Adsorption isotherms for CO_2 at different temperatures.

4 Sensitivity Analysis of the Convergence

To check the convergence of the simulations, we increased the simulation time from 50 000 to 500 000 steps. The error bars at the drop in the isobar remain high, indicating that they are inherent to the step itself. The CO_2/H_2O selectivity is smoother right after the step, but has the same behavior. The error bars on the CO_2/H_2O selectivity were estimated from a first-order Taylor expansion:

$$\frac{CO_2 \pm \Delta CO_2}{H_2O \pm \Delta H_2O} = \frac{CO_2}{H_2O} + \left(1 \pm \frac{\Delta CO_2}{CO_2} \mp \frac{\Delta H_2O}{H_2O}\right) \tag{10}$$

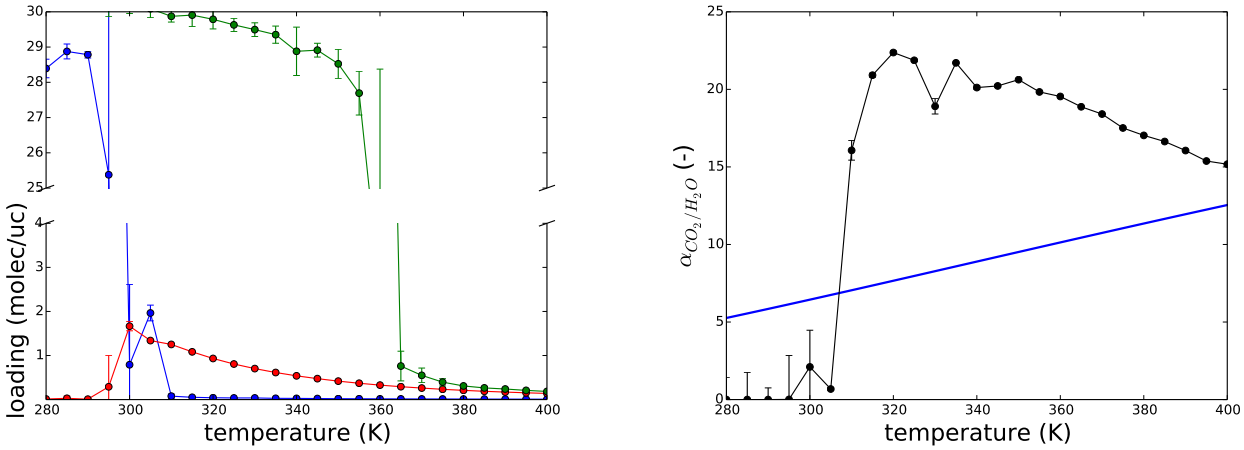

(a) Isobars

(b) CO_2/H_2O selectivity

Fig. 7 Isobars and selectivity when the simulation time is increased from 50 000 to 500 000 steps.

5 Force Field Parameters

	ε/k_b K	σ $Å$		ε/k_b K	σ $Å$
C_{CO_2}-C_{CO_2}	29.933	2.745			
C_{CO_2}-O_{CO_2}	50.640	2.880	O_{spce}-O_{spce}	78.197	3.1656
O_{CO_2}-C_{CO_2}	85.617	3.017			
C_{CO_2}-O_{zeo}	37.595	3.511	O_{spce}-O_{zeo}	85.152	3.723
O_{CO_2}-O_{zeo}	78.980	3.237			
C_{CO_2}-Na	362.292	3.320	O_{spce}-Na	564.881	3.361
O_{CO_2}-Na	200.831	2.758			

Table 7 Lennard-Jones parameters used in this work. [10,11]

	charge
O	-0.393
O_a	-0.414
Si	0.786
Al	0.486
C	0.651
O	-0.326
Na	0.383
O	-0.848
H_{spce}	0.424
N_{n2}	-0.405
N_{com}	0.810

Table 8 Charges on the atoms. [10,11]

6 Sensitivity of the post-Pareto Search

To check the sensitivity of the post-Pareto algorithm, we vary the importance of the different criteria (Table 9). We argue that the CO_2/H_2O and CO_2/N_2 selectivities are the most important metrics, that the CO_2 uptake is half as important (to avoid the construction of too big an adsorption column) and that the H_2O uptake is 10 times less important than the selectivity (provided that enough H_2O is available). For this specific case, we obtain the Pareto skyline in Figure 8 and minimum win fractions in Table 10. We observe that there is only a limited influence on the minimum win fraction of the materials in the Pareto set.

property	unit	weight	objective
α_{CO_2/H_2O}	(-)	10	max
α_{CO_2/N_2}	(-)	10	max
$N_{CO_2,400K}$	molecules/nm^3	5	max
$N_{H_2O,300K}$	molecules/nm^3	1	min

Table 9 Properties optimized with the Pareto approach, the units, their relative weights and the objective (to maximize or to minimize the criterium)

	mwf (-)		mwf (-)
STW	52.9%	IHW	1.0%
AEL	47.1%	TER	0.6%
EAB	13.3%	VET	0.4%
AWW	13.0%	PAU	0.3%
UFI	10.9%	CAN	0.2%
LEV	10.4%	ATO	0.2%
STI	5.3%	MTT	0.1%
RTE	3.6%	TON	0.1%
MTF	3.3%	AFO	0.1%
LTF	1.3%		

Table 10 Minimum win fractions for the materials in the Pareto set, with respect to the CO_2/H_2O selectivity, the CO_2/N_2 selectivity and the CO_2 uptake at 400 K of the binary mixture and the H_2O uptake at 300 K and 100 kPa

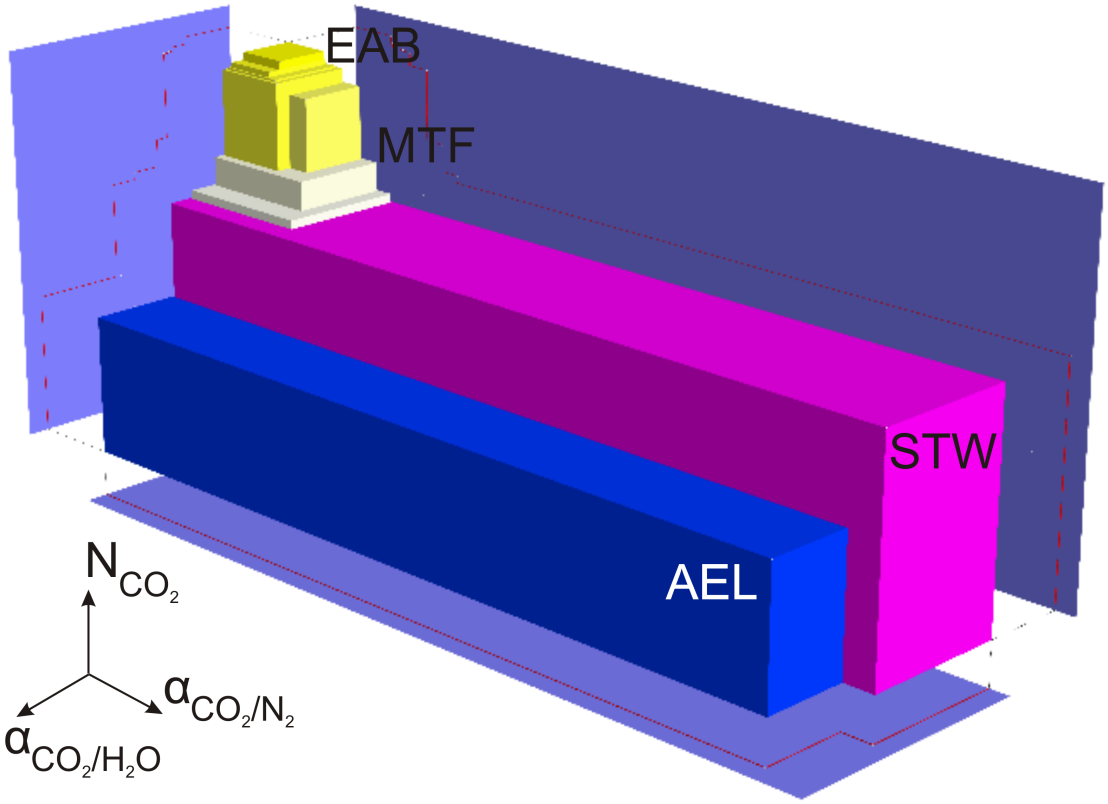

Fig. 8 Skyline plot and the projection on the CO_2/H_2O and CO_2/N_2 selectivity and the CO_2 uptake.

7 Post-Pareto Search at Different Temperatures

	mwf (-)		mwf (-)
AEL	54.1 %	PAU	2.5 %
BOF	45.9 %	VET	1.9 %
STW	43.2 %	ATO	1.7 %
ESV	32.3 %	MTT	1.4 %
FER	13.0 %	TON	1.2 %
UFI	8.6 %	AFO	0.5 %

Table 11 Post-Pareto analysis for adsorption at 325 K: Minimum win fractions for the materials in the Pareto set, with respect to the CO_2/H_2O selectivity, the CO_2/N_2 selectivity and the CO_2 uptake at **325 K** of the binary mixture and the H_2O uptake at 300 K and 100 kPa

	mwf (-)		mwf (-)
AEL	59.0%	VET	1.9 %
BOF	41.0 %	ATO	1.8 %
STW	39.9 %	MTT	1.4 %
ESV	35.4 %	TON	1.3 %
FER	17.3 %	PAU	0.9 %
UFI	3.4 %	AFO	0.5 %

Table 12 Post-Pareto analysis for adsorption at 350 K: Minimum win fractions for the materials in the Pareto set, with respect to the CO_2/H_2O selectivity, the CO_2/N_2 selectivity and the CO_2 uptake at **350 K** of the binary mixture and the H_2O uptake at 300 K and 100 kPa

	mwf (-)		mwf (-)
AEL	59.8 %	PAU	2.1 %
STW	40.2 %	VET	1.9 %
BOF	38.3 %	ATO	1.8 %
ESV	36.2 %	MTT	1.4 %
LAU	4.6 %	TON	1.3 %
MTF	4.1 %	AFO	0.5 %

Table 13 Post-Pareto analysis for adsorption at 375 K: Minimum win fractions for the materials in the Pareto set, with respect to the CO_2/H_2O selectivity, the CO_2/N_2 selectivity and the CO_2 uptake at **375 K** of the binary mixture and the H_2O uptake at 300 K and 100 kPa

8 All Data at 400 K

name	ΔH_{CO_2}	ΔH_{H_2O}	α_{CO_2/H_2O} 300K	α_{CO_2/H_2O} 400K	α_{CO_2/N_2} 300K	α_{CO_2/N_2} 400K	N_{CO_2} 400K	N_{H_2O} 400K
	kJ/mol	kJ/mol	-	-	-	-	molec/nm^3	molec/nm^3
AEI	-22.6	-36.6	0.0652	8.9836	7.4929	4.6181	0.0343	7.0940
AEL	-27.9	-29.4	20.1686	20.9701	140.8229	49.6913	0.0326	3.2817
AET	-17.3	-31.7	0.0004	6.1701	3.9502	2.7285	0.0095	5.9299
AFI	-19.3	-33.8	0.0015	7.5146	4.4481	3.0657	0.0178	6.5526
AFN	-27.5	-25.8	44.2409	17.5982	180.6743	58.2215	0.0178	0.5330
AFO	-27.3	-31.2	0.2503	15.5295	61.5568	25.2739	0.0326	3.2247
AFR	-20.4	-30.8	0.0036	6.9206	6.3061	3.5904	0.0191	8.3217
AFS	-19.7	-31.4	0.0026	6.8750	6.9609	4.0327	0.0181	10.1182
AFT	-23.3	-34.9	0.1069	9.0672	8.4536	4.6223	0.0304	6.8610
AFX	-23.9	-33.3	0.2914	9.4046	9.0779	4.5193	0.0284	7.1540
AFY	-21.0	-31.4	0.0030	7.6322	11.6244	5.6325	0.0187	10.8279
ASV	-28.5	-24.2	16.4386	9.4059	120.6240	42.9403	0.0215	4.7488
ATN	-31.2	-22.4	34.0389	14.5570	126.1242	38.7922	0.0413	0.4038
ATO	-25.8	-30.9	0.0600	11.4804	24.7083	12.5961	0.0265	2.9365
ATS	-20.5	-32.2	0.0045	7.9354	6.0689	3.7973	0.0207	6.5761
ATT	-31.3	-21.5	53.5375	19.3091	547.4386	118.1499	0.0256	0.1664
AWO	-27.2	-25.6	3.2928	2.7025	3979.8283	534.9081	0.0026	0.2227
AWW	-25.9	-37.3	1.5800	10.3898	9.6899	5.5888	0.0598	5.9778
BEC	-21.0	-31.6	0.0003	7.5444	5.9434	3.8889	0.0315	8.3449
BOF	-28.6	-26.7	16.8459	15.0569	127.3299	45.8504	0.0423	4.7582
BOG	-22.0	-30.9	0.0005	8.3071	7.8403	4.1126	0.0241	8.9036
BPH	-20.3	-31.6	0.0041	6.6464	6.4352	3.7605	0.0196	10.1277
BSV	-27.8	-19.2	30.5470	13.7269	5037.8137	746.7935	0.0064	0.0470
CAN	-24.1	-32.7	0.0000	10.5129	11.9499	7.0728	0.0270	2.8362
CDO	-28.5	-21.3	23.6945	11.2737	52.5954	23.2312	0.0261	0.2866
CFI	-18.7	-33.4	0.0001	7.2783	4.4346	3.0379	0.0135	6.3315
CGS	-26.8	-21.4	25.5653	13.1747	35.1584	16.3055	0.0297	1.4530
CHA	-22.7	-34.6	0.4193	9.0758	7.7344	4.7931	0.0359	6.4698
DDR	-25.0	-38.6	0.3621	10.8781	8.5817	5.0666	0.0367	3.8467
DFO	-21.5	-28.3	0.0008	7.6132	7.7323	4.2885	0.0244	9.8812
DON	-17.3	-30.7	0.0002	6.2281	3.8451	2.6473	0.0116	6.9205
EAB	-27.5	-34.8	0.8752	11.9207	15.7427	7.0302	0.0583	4.6404
EDI	-27.9	-20.6	19.8092	9.9483	137.5728	46.5274	0.0186	0.2292
EMT	-16.1	-30.5	0.0002	5.2841	3.7326	2.5441	0.0121	12.1918
EON	-28.3	-32.6	0.1206	10.1544	15.3957	6.1258	0.0332	4.8596
EPI	-30.1	-23.5	27.5800	13.8327	353.9683	96.3856	0.0301	0.5011
ERI	-23.8	-32.5	0.8317	9.5625	7.9922	4.9005	0.0419	6.3362
ESV	-29.0	-26.2	14.6052	13.8226	22.9953	10.6084	0.0621	2.8253
ETR	-26.7	-28.3	0.0470	14.5834	14.1259	6.8546	0.0249	6.6319
EUO	-24.4	-31.7	0.1361	10.6370	10.7725	6.0497	0.0317	6.2468
EZT	-23.9	-33.5	0.0078	9.4499	9.7043	5.6680	0.0376	5.0385
FAU	-15.1	-29.4	0.0003	5.2391	3.5639	2.4728	0.0112	12.2162
FER	-28.5	-24.1	15.4023	13.5978	29.5371	15.4189	0.0482	3.5879
GIS	-30.7	-17.4	178.4244	43.3283	21368.4646	2000.8397	0.0131	0.0257
GME	-25.8	-34.1	0.0527	9.7764	12.2073	4.3153	0.0219	6.2312

name	ΔH_{CO_2}	ΔH_{H_2O}	α_{CO_2/H_2O} 300K	α_{CO_2/H_2O} 400K	α_{CO_2/N_2} 300K	α_{CO_2/N_2} 400K	N_{CO_2} 400K	N_{H_2O} 400K
	kJ/mol	kJ/mol	-	-	-	-	molec/nm^3	molec/nm^3
GON	-23.8	-34.6	0.0040	10.3338	12.4738	7.2548	0.0246	3.6790
HEU	-29.3	-22.8	30.1873	14.3607	62.7414	25.6080	0.0345	1.0382
IFR	-23.1	-32.8	0.0105	9.0577	7.1212	4.3498	0.0417	7.2967
IHW	-25.6	-33.3	2.8861	12.2721	12.6481	7.0424	0.0396	3.4397
IMF	-25.5	-31.5	0.0046	10.3845	20.3210	9.7919	0.0365	5.8673
ISV	-20.3	-31.8	0.0005	7.2874	5.5953	3.6704	0.0277	8.7477
ITE	-22.1	-35.2	0.0039	8.3601	6.5618	4.0598	0.0331	7.4774
ITH	-25.0	-32.8	0.0071	10.6997	21.8634	11.1303	0.0295	5.4643
ITR	-24.8	-30.6	0.0027	10.2622	19.3698	10.2391	0.0304	5.1353
IWR	-21.8	-31.9	0.0012	8.4000	7.7287	4.6059	0.0307	9.1136
IWS	-19.6	-31.9	0.0003	6.5838	5.2156	3.4010	0.0228	10.4712
IWV	-18.1	-30.8	0.0007	6.0109	4.6714	2.9504	0.0158	10.2082
IWW	-23.2	-31.7	0.0019	9.0431	10.0140	5.7246	0.0305	6.7316
KFI	-24.8	-29.6	0.0694	10.6100	13.4417	5.8798	0.0307	8.2343
LAU	-27.4	-27.0	12.1067	11.8778	23.2728	11.7438	0.0460	4.5510
LEV	-25.5	-31.3	2.8874	11.2501	9.7467	5.7046	0.0589	5.9771
LTA	-18.5	-31.6	0.0004	6.7443	4.6430	3.0435	0.0192	10.0641
LTF	-28.9	-30.5	0.2020	11.5151	20.1110	8.0552	0.0413	3.4208
LTL	-21.3	-31.0	0.0016	6.1951	8.8636	4.0910	0.0141	6.8857
MAZ	-29.2	-29.3	0.1445	11.6619	19.2554	7.4150	0.0427	4.4249
MEI	-20.9	-31.3	0.0049	6.6487	7.6620	4.1160	0.0207	9.5433
MEL	-24.9	-32.0	0.0003	10.0036	17.3636	8.4914	0.0343	6.0633
MER	-25.3	-25.5	25.2079	14.7131	22.1987	11.9153	0.0206	0.8168
MFI	-26.6	-31.9	3.8096	15.3350	36.5937	16.7037	0.0285	5.7260
MFS	-24.3	-34.7	0.0087	10.2395	13.0612	7.3642	0.0290	4.7287
MOR	-21.1	-31.0	0.0068	7.4345	6.3082	4.1807	0.0175	4.4696
MOZ	-25.9	-30.0	0.0656	9.3848	11.5813	5.7059	0.0332	5.7111
MSE	-22.0	-30.8	0.0005	8.7183	6.9239	4.5139	0.0334	6.9035
MTF	-28.3	-36.3	2.3209	14.3035	22.4006	10.7215	0.0448	3.7383
MTT	-26.5	-30.6	12.2325	14.6270	32.5834	15.4110	0.0282	3.0571
MTW	-24.0	-35.2	0.0006	10.4255	13.4214	7.3534	0.0233	3.9007
MWW	-25.1	-34.7	0.0042	9.4840	12.0700	6.1452	0.0371	8.9206
NES	-22.3	-32.3	0.0010	9.0924	9.0353	5.4123	0.0287	7.0150
OBW	-22.1	-30.8	0.0150	7.3767	9.0974	4.2246	0.0172	8.4267
OSI	-21.7	-33.1	0.0008	9.3062	7.4100	4.7408	0.0184	3.8522
OSO	-20.1	-31.6	0.0684	8.5235	10.7020	6.4297	0.0195	9.0030
OWE	-28.5	-25.6	20.1065	11.9688	44.9345	19.0377	0.0390	1.9847
PAU	-26.2	-34.6	0.5592	13.7652	20.2916	9.6060	0.0239	2.7034
PHI	-28.6	-19.6	52.3177	20.7669	212.2299	65.8758	0.0225	0.1159
PON	-28.7	-24.4	76.5565	26.6038	4641.4734	770.1147	0.0141	0.3503
PUN	-24.6	-21.9	29.9870	14.7585	73.1460	31.5224	0.0228	7.8591
RHO	-18.7	-32.0	0.0017	7.0257	4.9097	3.1504	0.0173	8.9168
RTE	-26.4	-32.6	3.6816	11.5433	11.8896	6.5032	0.0584	5.8017
RTH	-22.5	-36.4	0.0045	8.9009	6.8585	4.1834	0.0356	8.0349
RWY	-13.1	-23.6	0.3742	4.5327	3.1343	2.1987	0.0091	19.7531
SAF	-21.1	-34.1	0.0014	8.1301	6.1431	4.0103	0.0186	3.7489

name	ΔH_{CO_2}	ΔH_{H_2O}	α_{CO_2/H_2O} 300K	α_{CO_2/H_2O} 400K	α_{CO_2/N_2} 300K	α_{CO_2/N_2} 400K	N_{CO_2} 400K	N_{H_2O} 400K
	kJ/mol	kJ/mol	-	-	-	-	molec/nm^3	molec/nm^3
SAO	-18.1	-30.7	0.0004	6.4167	4.2327	2.9813	0.0224	11.9300
SAS	-20.8	-35.1	0.0027	7.7509	5.4060	3.4757	0.0305	8.6193
SAT	-24.2	-32.4	0.6634	9.1197	8.6281	5.2340	0.0411	4.6787
SAV	-23.0	-33.3	0.0439	9.2310	9.1031	4.7482	0.0283	7.3659
SBE	-21.4	-30.8	0.0051	5.7456	6.5285	2.5944	0.0123	11.3858
SBS	-17.1	-29.5	0.0003	5.7324	4.4593	2.7591	0.0135	12.4156
SBT	-17.2	-27.7	0.0002	5.7569	4.4773	2.7538	0.0137	12.2922
SFE	-20.8	-33.5	0.0009	8.5518	7.6876	4.6303	0.0185	5.1250
SFF	-23.1	-35.5	0.0055	8.9412	7.4411	4.5660	0.0379	6.7172
SFG	-23.7	-34.1	0.0041	9.2600	11.3426	6.3556	0.0261	4.9209
SFH	-18.6	-31.4	0.0017	7.2105	4.9387	3.1761	0.0136	7.2645
SFN	-18.6	-32.3	0.0003	7.1364	5.1882	3.3359	0.0137	7.2065
SFO	-20.5	-31.8	0.0067	7.0439	6.3553	3.5450	0.0193	8.7957
SFS	-23.9	-31.5	0.0009	8.8269	12.4112	5.5703	0.0265	7.4930
SIV	-29.6	-19.2	78.2754	26.6561	399.5302	109.9447	0.0178	0.0697
SOF	-24.9	-30.3	48.6684	23.6119	380.9667	111.7157	0.0173	7.1467
SOS	-23.5	-21.2	55.7553	28.4799	3025.2134	571.3229	0.0050	0.0229
SSF	-19.3	-31.6	0.0005	7.2659	4.9257	3.3572	0.0182	6.6079
SSY	-20.8	-33.3	0.0462	8.5667	7.0558	4.3243	0.0181	6.1897
STF	-22.9	-36.0	0.0021	8.6397	8.1613	4.7419	0.0355	8.1643
STI	-25.6	-26.9	0.9716	12.6327	17.9836	9.6275	0.0481	5.2172
STT	-24.3	-35.8	0.2027	9.8649	9.5190	5.4077	0.0413	7.1373
STW	-26.9	-30.8	1.4072	15.7792	156.9842	51.5893	0.0439	7.2589
SZR	-25.0	-38.0	1.4491	11.3104	16.8063	9.2597	0.0249	3.8699
TER	-25.3	-30.1	0.0130	11.5781	23.6987	11.3075	0.0344	6.2266
THO	-27.7	-19.6	39.6730	14.7470	622.3710	155.0300	0.0146	0.0983
TON	-26.5	-31.6	0.4532	13.0439	56.4313	23.2297	0.0278	3.1028
TSC	-16.4	-31.5	0.0002	5.5529	4.0198	2.6143	0.0103	11.8264
TUN	-25.6	-31.8	0.0005	10.6541	18.8982	8.8032	0.0354	6.2426
UEI	-26.7	-22.3	11.4575	7.1168	163.6494	54.8312	0.0064	0.1267
UFI	-32.3	-31.3	0.0987	11.0757	36.3474	8.3870	0.0567	8.1430
UOS	-26.6	-23.6	20.2902	13.6749	60.3032	27.5622	0.0203	5.1961
USI	-22.6	-33.3	0.0271	8.9460	9.0589	4.7986	0.0255	7.9272
UTL	-20.5	-32.6	0.0009	6.9358	6.0892	3.3793	0.0197	10.0870
VET	-23.1	-32.6	0.0183	9.6758	8.1352	5.1386	0.0215	2.5159
VFI	-13.8	-27.1	0.3451	4.8143	3.3049	2.2199	0.0063	10.7442
ZON	-31.0	-22.8	34.7212	15.4412	79.6306	28.4859	0.0522	0.4702

Table 14 Adsorption enthalpy for CO_2 and H_2O, CO_2/H_2O and CO_2/N_2 selectivities at 300 K and 400 K. CO_2 uptake under adsorption conditions (14 kPa CO_2, 6 kPa H_2O, 400 K) and H_2O uptake under desorption conditions (100 kPa H_2O and 300 K).

References

1 D. A. McQuarrie and J. D. Simon, *Physical Chemistry: A Molecular Approach, Volume 1*, University Science Books, 1997.

2 G. Kresse and D. Joubert, *Phys. Rev. B*, 1999, **59**, 1758–1775.

3 G. Kresse, a. Gil and P. Sautet, *Phys. Rev. B*, 2003, **68**, 073401.

4 B. Hammer, L. Hansen and J. Nørskov, *Phys. Rev. B*, 1999, **59**, 7413–7421.

5 J. P. Perdew, K. Burke and M. Ernzerhof, *Phys. Rev. Lett.*, 1996, **77**, 3865–3868.

6 S. Grimme, *Journal of Computational Chemistry*, 2004, **25**, 1463–1473.

7 C. Baerlocher and L. McCusker, *Database of Zeolite Structures*, 2014, `http://www.iza-structure.org/databases`.

8 E. Verheyen, L. Joos, K. Van Havenbergh, E. Breynaert, N. Kasian, E. Gobechiya, K. Houthoofd, C. Martineau, M. Hinterstein, F. Taulelle, V. Van Speybroeck, M. Waroquier, S. Bals, G. Van Tendeloo, C. E. A. Kirschhock and J. A. Martens, *Nature Materials*, 2012, **11**, 1059–1064.

9 M. J. Frisch, G. W. Trucks, H. B. Schlegel, G. E. Scuseria, M. A. Robb, J. R. Cheeseman, G. Scalmani, V. Barone, B. Mennucci, G. A. Petersson, H. Nakatsuji, M. Caricato, X. Li, H. P. Hratchian, A. F. Izmaylov, J. Bloino, G. Zheng, J. L. Sonnenberg, M. Hada, M. Ehara, K. Toyota, R. Fukuda, J. Hasegawa, M. Ishida, T. Nakajima, Y. Honda, O. Kitao, H. Nakai, T. Vreven, J. A. Montgomery, Jr., J. E. Peralta, F. Ogliaro, M. Bearpark, J. J. Heyd, E. Brothers, K. N. Kudin, V. N. Staroverov, R. Kobayashi, J. Normand, K. Raghavachari, A. Rendell, J. C. Burant, S. S. Iyengar, J. Tomasi, M. Cossi, N. Rega, J. M. Millam, M. Klene, J. E. Knox, J. B. Cross, V. Bakken, C. Adamo, J. Jaramillo, R. Gomperts, R. E. Stratmann, O. Yazyev, A. J. Austin, R. Cammi, C. Pomelli, J. W. Ochterski, R. L. Martin, K. Morokuma, V. G. Zakrzewski, G. A. Voth, P. Salvador, J. J. Dannenberg, S. Dapprich, A. D. Daniels, . Farkas, J. B. Foresman, J. V. Ortiz, J. Cioslowski and D. J. Fox, *Gaussian 09 Revision D.01*, Gaussian Inc. Wallingford CT 2009.

10 A. García-Sánchez, C. O. Ania, J. B. Parra, D. Dubbeldam, T. J. H. Vlugt, R. Krishna and S. Calero, *The Journal of Physical Chemistry C*, 2009, **113**, 8814–8820.

11 L. Joos, J. A. Swisher and B. Smit, *Langmuir*, 2013, **29**, 15936–15942.